

Experimental and theoretical approaches on mechanical evaluation of Y123 system by Lu addition

M. B. Turkoz · S. Nezir · O. Ozturk ·
E. Asikuzun · G. Yildirim · C. Terzioglu ·
A. Varilci

Received: 27 December 2012 / Accepted: 29 January 2013 / Published online: 5 February 2013
© The Author(s) 2013. This article is published with open access at Springerlink.com

Abstract This work is the continuation of a systematic study on the characterization of the Lu-added Y123 bulk superconducting materials prepared by the nitrate compounds and derivatives at 970 °C for 20 h. In this part, the effect of Lu inclusions on the physical and mechanical properties of the Y123 superconductors is examined with the aid of microhardness measurements performed at various applied loads in the range of 0.245–2.940 N. The microhardness measurement results allow us to determine the important mechanical characteristics such as Vickers microhardness, elastic (Young's) modulus, yield strength and fracture toughness values being responsible for the potential industrial applications. It is found that all the properties given above are strongly dependent upon the Lu concentration in the Y123 matrix. Especially, Vickers microhardness (H_v) values of the samples studied in this work are found to be suppressed considerably with the enhancement of the Lu addition in the system due to the degradation in the connectivity between superconducting grains. Moreover, the H_v values of the pure Y123 sample are observed to increase with increasing the applied load whereas those of the Lu-doped superconducting materials are obtained to decrease with the load. In other words, the

pure sample exhibits the reverse indentation size effect (RISE) behavior while the others obey the indentation size effect (ISE) feature, confirming the degradation in the mechanical properties with the Lu inclusions in the Y123 matrix. In addition, the microhardness measurement results are estimated using the 5 different models such as Meyer's law, proportional sample resistance model, elastic/plastic deformation model, Hays–Kendall (*HK*) approach and indentation-induced cracking (*IIC*) model. According to the results obtained from the simulations, of the mechanical analysis models, the Hays–Kendall (*HK*) approach is determined as the most successful model for the description of the mechanical properties of the Lu-doped superconducting materials (exhibiting the *ISE* behavior) where both the reversible (elastic) and irreversible (plastic) deformations are produced. On the other hand, the *IIC* model is found to be superior to other approaches for the pure sample (presenting the *RISE* feature) where the irreversible deformation becomes more and more dominant compared to the reversible deformation.

1 Introduction

$\text{YBa}_2\text{Cu}_3\text{O}_{7-\delta}$ high-temperature superconducting ceramic being composed of a perovskite structure with bent Cu–O chains [1] has the critical temperature of 92 K [2] and is referred to as Y123 superconductor due to the relative numbers of metal atoms in the chemical formula [3]. Moreover, Y123 is the first known material obtaining a superconducting transition temperature above liquid nitrogen temperature (77 K) [3, 4]. Thus, the Y123 material is the most candidate superconductor for the potential applications in technology and industry with their remarkable smaller power losses, high current and magnetic field

M. B. Turkoz (✉) · S. Nezir
Department of Physics Faculty of Arts and Science,
Kırıkkale University, 71450 Kırıkkale, Turkey
e-mail: turkozmb@gmail.com

O. Ozturk · E. Asikuzun
Department of Physics Faculty of Arts and Science,
Kastamonu University, 37100 Kastamonu, Turkey

G. Yildirim · C. Terzioglu · A. Varilci
Department of Physics Faculty of Arts and Science,
Abant İzzet Baysal University, 14280 Bolu, Turkey

carrying capacity, optical and electronic properties [5–9]. Further, the simple chemical composition, easy availability of the starting powders, low material cost, simplicity of the synthesis procedure, high T_c value, low resistivity near T_c and nontoxicity characteristics (compared to Tl and Hg-based superconductors) allow the Y123 material was used in the practical applications [10–12]. Nevertheless, due to the inherent brittle structure of the ceramic material, the surface of the Y123 sample is vulnerable to excessive stress, leading to a factor restricting high stress mechanical applications.

It is well known that the microhardness of a solid depends on the applied load [13–15]. This phenomenon is known as indentation size effect (*ISE*) behavior, explaining the decrement in the hardness with the enhancement of the applied load. This behavior may stem from several factors such as temperature, elastic and plastic deformations, indentation size, friction of the indenter and level of cracks/voids [16–22]. The opposite term of ISE is called as reverse *ISE* (*RISE*) behavior, being described by the increment in the microhardness value with the applied load. In this present study, we explore the effect of the Lu inclusions in the Y123 matrix on the mechanical properties with the aid of the microhardness measurements. Moreover, Vickers microhardness, elastic (Young's) modulus, yield strength and fracture toughness values are estimated from the microhardness curves. It is observed that the properties given above depend on sensitively on the Lu concentration and applied load. The results of the microhardness measurements are examined by 5 different available models such as Meyer's law, proportional sample resistance, elastic/plastic deformation, Hays–Kendall and indentation-induced cracking (*IIC*) model. According to the findings obtained, the HK approach, among the models studied in this work, is found to be the best model describing the microhardness of the Lu-doped Y123 bulk superconductors exhibiting the ISE behavior whereas the *IIC* model is noted to be superior to other approaches for the pure sample presenting the *RISE* feature.

2 Experimental details

In previous works [23, 24], we reported the change of the microstructural and superconducting properties of Lu-doped Y123 superconducting samples with the aid of X-ray diffraction analysis, scanning electron microscopy, electron dispersive X-ray, electrical resistivity and transport critical current density measurements as well as examining the flux pinning mechanism properties in the applied magnetic fields range of 0–6 kG. In the present work, using the same samples, the role of Lu inclusions in the Y123 matrix on mechanical properties is explored by

Vickers microhardness (H_v) measurements being performed at room temperature with Shimadzu HVM-2 model digital microhardness tester. The applied load is varied from 0.245 to 2.940 N for a loading time of 10 s and accuracy in the determination of indentation diagonals is measured to be $\pm 0.1 \mu\text{m}$. The indenter is pressed on the different locations on the specimen surface to avoid surface effects and work hardening. For each applied load, the reasonable mean values are determined from the average of five readings at different locations of the specimen surfaces. The microhardness results obtained enable us to deduce some important mechanical properties (Vickers microhardness, elastic modulus, yield strength and fracture toughness) for the industrial applications of the superconducting materials. Moreover, the experimental results of the microhardness measurements are analyzed by 5 different methods such as Meyer's law, PSR, MPSR, EPD, Hays–Kendall and IIC models, and the most successful model describing the Vickers microhardness of Y123 superconducting samples is also discussed clearly in the text. The $\text{YBa}_2\text{Lu}_x\text{Cu}_3\text{O}_{7-\delta}$ superconducting samples with $x = 0, 0.1, 0.3, 0.5$ and 0.7 will be herein after visualized as Lu0.0, Lu0.1, Lu0.3, Lu0.5 and Lu0.7, respectively.

3 Results and discussion

3.1 Microhardness and modeling

As well known the measurement of the hardness is the most general experiment to analyze the mechanical properties of a material as a result of the simple measurement system and less damage to the specimen surface. Other important advantage of the hardness measurement enables us to obtain the other mechanical properties such as elastic modulus, yield strength, brightness index and fracture toughness. Moreover, the hardness being named as resistance towards to the plastic deformation, slipping and friction is a measurement method. The value of the hardness measurements performed at the laboratory by means of the specific tools is the resistance against the plastic (irreversible) deformation. In other words, the hardness is to measure the resistance appeared in the material due to the immersion of the rigid (diamond) indenter on the specimen surface. The selected indenter leaves a trace as immersed on specimen surface. In general terms, the hardness of the material is inversely proportional to the size of indentation. In this study, the load in range from 0.245 to 2.940 N for a loading time of 10 s is applied on the Lu doped-Y123 superconducting samples. After the indenter is removed from the sample surface, the indentation diagonal sizes are determined and the Vickers microhardness values are calculated from Eq. 1.

$$H_V = 1854.4 \left(\frac{F}{d^2} \right) (\text{GPa}) \quad (1)$$

where F denotes the applied load, and d is the average of the indentation diagonal sizes $(d_1 + d_2)/2$. Depending on the microhardness, the elastic modulus, yield strength and fracture toughness values are derived by the relations given below:

$$E = 81.9635H_V \quad (2)$$

$$Y \approx \frac{H_V}{3} \quad (3)$$

$$K_{IC} = \sqrt{2E\gamma} \quad (\gamma, \text{ surface energy}) \quad (4)$$

The load dependent microhardness (H_V), elastic modulus (E), yield strength (Y) and fracture toughness (K_{IC}) values for the samples are depicted in Table 1. It is apparent from the table that the Vickers microhardness values increase with the enhancement of the applied load whereas for the Lu-doped bulk Y123 superconducting materials the hardness values reduce with the applied load. According to results obtained, RISE behavior is more dominant in the pure sample while ISE behavior starts to be dominant with the presence of the Lu inclusions in the Y123 matrix. The decrement in the hardness value of the materials exhibiting the ISE behavior with the addition level and applied load is related to the grain boundary weak-links and impurity phases. Additionally, elastic modulus stems from the change of the material shape under the applied load. Table 1 depicts the decrement in the elastic modulus with the addition, which is the expectation state as a consequence of the reduction in the Vickers hardness values. Similar to the elastic modulus, yield strength values begin to degrade with the increase of the Lu addition in the Y123 system. This is attributed to the enhancement of the weak-links between the superconducting grains in the material. As for the fracture toughness being important parameter for the industrial applications of the material, the similar trend (decrease with the Lu individuals) is observed. Figure 1 shows the applied load dependent microhardness values. It is visible from the figure that the microhardness values belonging to the pure sample increase with the applied load whereas those of the Lu-doped samples decrease with the load. The curves of the hardness values reach to the plateau region at about 1 N for all the samples studied, meaning that there exists the important change on the microhardness values beyond the certain load value of 1 N. All the results obtained show the presence of the relationship between the applied load and microhardness of the solids. This relationship in the literature is known as Indentation Size Effect (ISE) nature, explaining that the hardness values decrease with the applied loads [25]. In contrast, the microhardness values sometimes increase with the

Table 1 The calculated load dependent H_V , E , Y and K_{IC} for the superconducting samples

Samples	Load (N)	d (μm)	H_V (GPa)	E (GPa)	Y (GPa)	K_{IC} ($\text{Pa}/\text{m}^{1/2}$)
Pure	0.245	16,35	1.699	139.26	0.566	1,574.4
	0.490	19,00	2.517	206.30	0.839	1,916.2
	0.980	26,04	2.680	219.66	0.893	1,977.3
	1.960	36,51	2.730	223.76	0.910	1,995.7
	2.940	44,72	2.742	224.74	0.914	2,000.9
Lu 0.1	0.245	13,06	2.663	218.27	0.887	1,549.5
	0.490	21,84	1.905	156.14	0.635	1,310.6
	0.980	31,30	1.854	151.96	0.618	1,292.9
	1.960	44,95	1.817	148.93	0.605	1,279.9
	2.940	54,96	1.804	147.86	0.601	1,275.3
Lu 0.3	0.245	13,28	2.576	211.14	0.858	1,755.7
	0.490	23,38	1.662	136.22	0.554	1,410.3
	0.980	33,79	1.591	130.40	0.530	1,379.8
	1.960	48,99	1.514	124.09	0.504	1,346.0
	2.940	60,32	1.498	122.78	0.499	1,338.9
Lu 0.5	0.245	19,15	1.238	101.47	0.412	1,290.0
	0.490	29,60	1.037	84.996	0.345	1,180.7
	0.980	51,41	0.687	56.309	0.229	960.97
	1.960	75,14	0.643	52.703	0.214	929.69
	2.940	93,62	0.622	50.981	0.207	914.38
Lu 0.7	0.245	21,58	0.976	79.996	0.325	1,004.0
	0.490	38,59	0.611	50.080	0.203	794.36
	0.980	56,04	0.580	47.539	0.193	773.94
	1.960	86,00	0.493	40.408	0.164	713.54
	2.940	107,16	0.475	38.933	0.158	700.39

enhancement of the applied load and this behavior is called as Reverse Indentation Size Effect (RISE). ISE behavior appearing in the material can be elucidated by means of the elastic–plastic deformation effect and friction of the indenter. On the other hand, RISE behavior is due to the specimen cracking/porosity and disorder, impurity phases and irregular grain orientation distribution. Thereby, the ISE and RISE behavior can be explained by 5 models given below.

3.2 Analysis according to Meyer's law

This approach is the simplest model to describe the Vickers microhardness of a material exhibiting the ISE behavior and the relationship between the applied load (F) and the indentation size (d) can be explained by means the following equation:

$$F = A_1 d^n \quad (5)$$

where power n being evaluated as a measurement of the ISE behavior shows Meyer number and A_1 denotes the

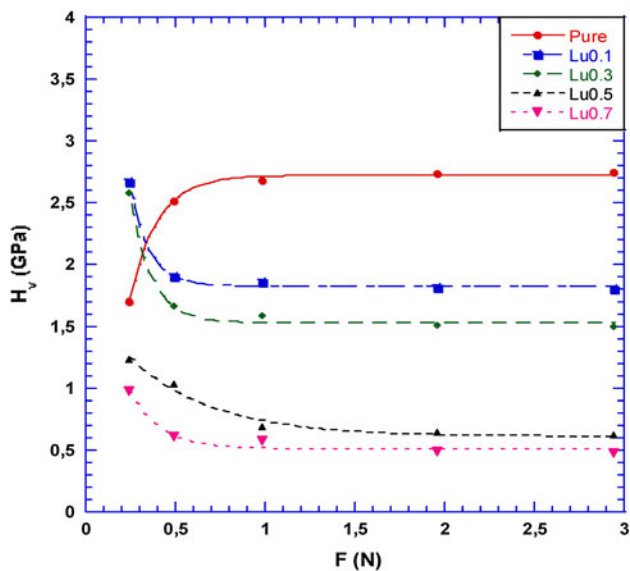


Fig. 1 Variation of load dependent microhardness H_v with applied load F

standard hardness constants. When the power n value is higher than 2, the material studied obeys the RISE behaviour. In contrast, if the Meyer number is less than 2, the material exhibits the ISE feature. Additionally, it is well known that Kick’s law is valid when the Meyer number is equal to 2, meaning that the hardness is independent upon the applied load [26–29]. Figure 2 illustrates the plots of $\ln F$ versus $\ln d$ for all the samples prepared. The slope of the $\ln F$ - $\ln d$ graph gives the value of n when the vertical intercept of the graph signifies A_1 value. The n and

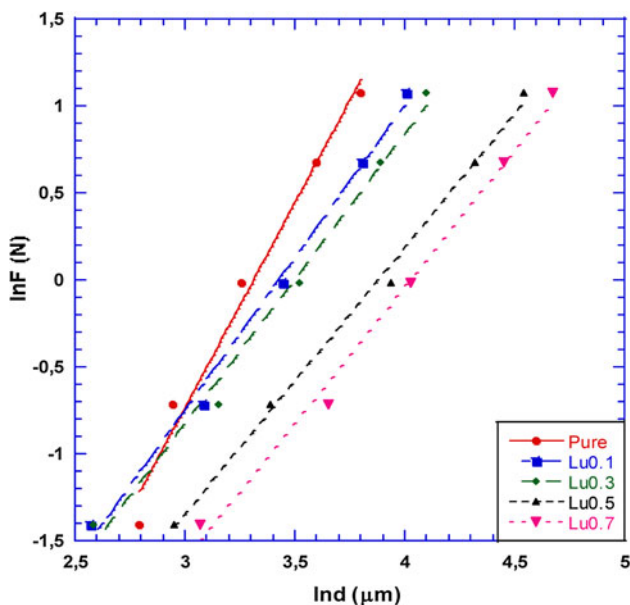


Fig. 2 Variation of applied load $\ln F$ with diagonal $\ln d$ for the samples

Table 2 Best-fit results of experimental data according to Meyer’s law

Samples	n_K	$\ln A_{1K}$ (GPa)	H_V (GPa)
Pure	2.35	-7.80	2.680–2.742
Lu0.1	1.74	-5.99	1.804–1.854
Lu0.3	1.66	-5.81	1.498–1.591
Lu0.5	1.53	-5.95	0.622–0.687
Lu0.7	1.56	-6.31	0.475–0.580

A_1 values obtained from the curves are summarized in Table 2. It is visible from the table that the n value is found to be greater than 2 for the Lu0.0 sample whereas the n value is observed to be less than 2 for the Lu-doped samples. This may be attributed to the fact that the load-dependent microhardness of the former sample obeys the RISE behavior (linear microhardness) while the microhardness of the latter samples decreases with the enhancement of the applied load (non-linear microhardness) [30].

3.3 Analysis according to PSR model

Proportional specimen resistance (PSR) approach is an alternative model to analyze the ISE behavior of a material. In this model, the ISE can be described by the following relation:

$$\frac{F}{d} = \alpha + \beta d \tag{6}$$

where α displays the surface energy stemming from the energy dispersion of the surface cracks. β parameter being independent upon the applied load is used to calculate the load independent microhardness. The values of α and β are determined from the F/d versus d graph as shown in Fig. 3. The results obtained are listed in Table 3. As seen from the table, the value of α is positive for the Lu0.1, Lu0.3, Lu0.5 and Lu0.7 samples showing the ISE behavior whereas it is negative for the virgin sample exhibiting RISE behavior, verifying that both the elastic and plastic deformations are produced in the Lu-doped samples [31–33]. In other words, there is no elastic (reversible) deformation for sample obeying RISE behavior.

Furthermore, the load independent microhardness value can be computed from the PSR model by the way of the following equation:

$$H_{PSR} = 1854.4\beta \tag{7}$$

Here, the load-independent H_{PSR} values are computed for each β parameter obtained. With the aid of Eqs. 4–6, we determine the load-independent Young’s (elastic) modulus, yield strength and fracture toughness values and list in Table 4. According to the table, the H_0 , E_0 and Y_0 values decrease with the increment in the Lu inclusions in the

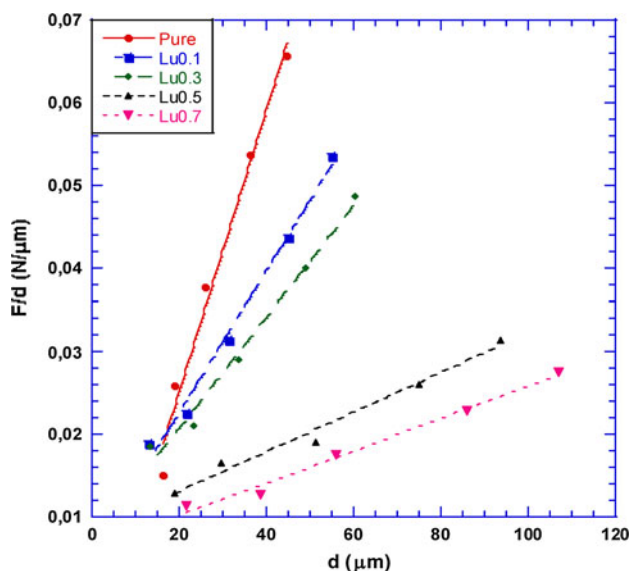


Fig. 3 Plots of F/d versus d for the samples

Table 3 Best-fit results of experimental data according to PSR model

Samples	$\alpha \times 10^{-2}$ (N/μm)	$\beta \times 10^{-3}$ (N/μm ²)	H_{PSR} (GPa)	H_V (GPa)
Pure	-0.89	1.70	3.152	2.680–2.742
Lu0.1	0.55	0.85	1.576	1.804–1.854
Lu0.3	0.73	0.66	1.223	1.498–1.591
Lu0.5	0.82	0.23	0.426	0.622–0.687
Lu0.7	0.63	0.19	0.352	0.475–0.580

Table 4 The calculated load independent H_0 , E_0 , Y_0 and K_{IC} for the samples

Samples	E_0 (GPa)	Y_0 (GPa)	K_{IC} (Pa/m ^{1/2})	H_V (GPa)
Pure	258.35	1.050	2,144.5	2.680–2.742
Lu0.1	129.17	0.525	1,192.0	1.804–1.854
Lu0.3	100.24	0.407	1,209.7	1.498–1.591
Lu0.5	34.91	0.142	756.72	0.622–0.687
Lu0.7	28.85	0.117	602.92	0.475–0.580

Y123 matrix. The Vickers microhardness values of the pure material exhibiting the RISE behavior are found to be greater than those of the Lu-doped samples presenting the ISE feature due to the lack of the elastic recovery [34–36]. In other words, the plastic as well as the elastic deformation is produced in the materials obeying the ISE behavior. It means that after the indenter is removed there is a relaxation on the specimen surface, leading to a decrement in the sample microhardness. The reduction of the elastic modulus, yield strength and fracture toughness along with the Vickers hardness is even an expectance result. Besides, as well known, the fracture toughness (K_{IC}) plays an

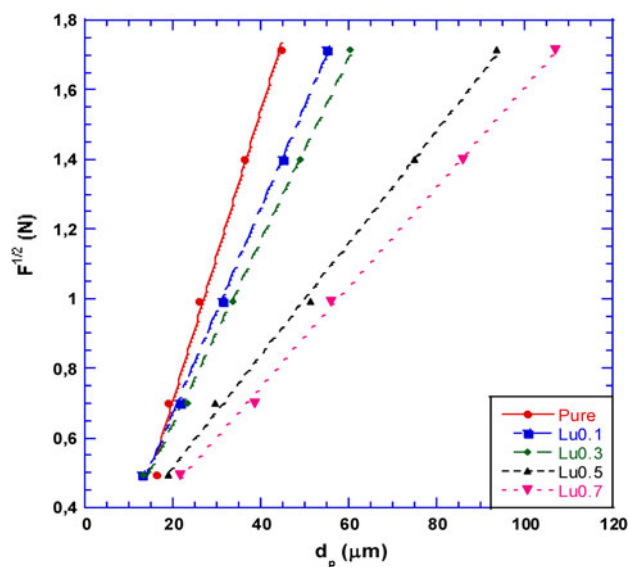


Fig. 4 Plots of diagonal length versus square root of applied loads for the samples

important role in the industrial applications. With the increase of the Lu concentration in the Y123 system, the K_{IC} value tends to decrease significantly due to the reduction of the surface energy α . Thus, it can be concluded that the Lu addition damages the mechanical properties of the Y123 superconducting system.

3.4 Analysis according to elastic/plastic deformation (EPD) model

Elastic/plastic deformation model is another useful approach to describe the superconducting materials exhibiting the ISE behavior. In the model the dependence of indentation size on the applied load is determined by the equation [37, 38]:

$$F = A_2(d_e + d_p)^2 \tag{8}$$

where A_2 gives the load independent hardness constant, and d_e (elastic deformation) is related to the d_p (plastic deformation). The values of d_e and A_3 are calculated by the variation of the square root of applied load ($F^{1/2}$) with the indentation size (d) as depicted in Fig. 4. Besides, the load independent microhardness value is computed by the use of the following relation.

$$H_{EPD} = 1854.4A_3 \tag{9}$$

All the values obtained are listed in Table 5. It is visible from the table that the value of d_e is found to be negative for the pure sample, meaning that there is not any clue on the elastic deformation in the material. The elastic recovery is observed for the Lu-doped bulk Y123 superconductors exhibiting the ISE behavior, confirming that both the

Table 5 Best-fit results of experimental data according to EPD model

Samples	A_2 (N/ μm^2)	d_e (μm)	H_{EPD} (GPa)	H_V (GPa)
Pure	0.041	-0.128	3.117	2.680–2.742
Lu0.1	0.029	0.082	1.559	1.804–1.854
Lu0.3	0.026	0.114	1.253	1.498–1.591
Lu0.5	0.016	0.193	0.474	0.622–0.687
Lu0.7	0.014	0.171	0.363	0.475–0.580

elastic and plastic deformations are produced in these samples under the applied load.

3.5 Analysis using Hays–Kendall approach

Observation of the ISE behavior in the microhardness tests performed by Hays–Kendall in 1973 for many different materials indicates that only elastic deformation appears below a certain limit of the applied load above which the plastic deformation begins to occur suddenly in the material studied [16]. In other words, the indenter can penetrate into the material beyond a certain load value named as the critical value of applied load [39]. Thus, the indentation size starts to increase after the critical applied load value of the material, and is proportional to an effective load $F_{eff} = F - W_{HK}$ instead of the applied load (Eq. 10).

$$F - W_{HK} = A_{1HK}d^2 \tag{10}$$

where A_{1HK} denotes the hardness constant independent of the applied load. The values of W_{HK} and A_{1HK} are obtained from F to d^2 graph for all the samples prepared. Furthermore, the load independent microhardness (H_{HK}) can be expressed using:

$$H_{HK} = 1854.4A_{1HK} \tag{11}$$

Hence, the slope of the plots given in Fig. 5 provides A_{1HK} value directly when the vertical intercept of the graph gives W_{HK} value. The H_{HK} value is calculated with the aid of Eq. 11. Table 6 tabulates the determined values of load independent microhardness H_{HK} , W_{HK} and A_{1HK} for all the samples. As seen from the table the value of W_{HK} is positive for the Lu-doped samples exhibiting the ISE behavior whereas the pure sample obeying the RISE feature obtains the negative value of W_{HK} . It may be attributed to the fact that the positive value is sufficient to produce the elastic (reversible) deformation as well as the plastic (irreversible) deformation in the materials. On the other hand, the negative value is due to dominant characterization of the plastic deformation in the system [40]. It is another important result obtained from Fig. 5 that the microhardness values determined with regard to HK model provide closer results to the ones in the plateau region as

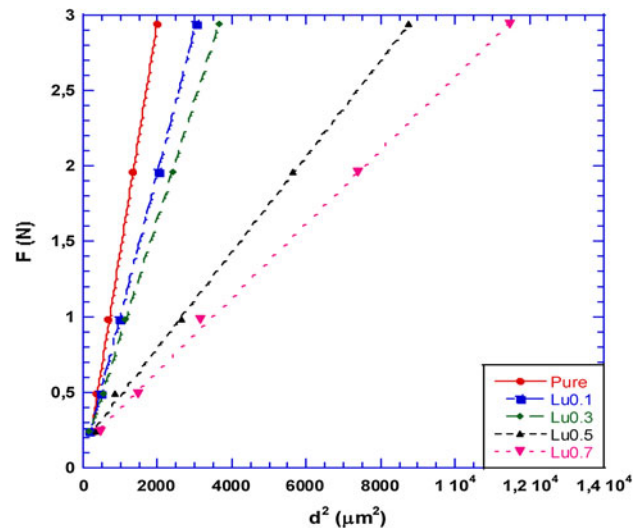


Fig. 5 Applied load versus the square of the impression semi-diagonal length for the samples

Table 6 Best-fit results of experimental data according to HK model

Samples	$A_{1HK} \times 10^{-5}$	W_{HK} (N)	H_{HK} (GPa)	H_V (Plateau Region) (GPa)
Pure	152.8	-0.095	2.833	2.680–2.742
Lu0.1	95.02	0.055	1.762	1.804–1.854
Lu0.3	78.31	0.085	1.452	1.498–1.591
Lu0.5	31.70	0.162	0.587	0.622–0.687
Lu0.7	24.38	0.153	0.452	0.475–0.580

compared to the results obtained from the other models. In the literature, the microhardness studies on various materials showed that the load independent microhardness values should be close to those at the plateau region [41–43]. Hence, it can be concluded that Hays–Kendall approach is the most suitable model for both the calculation of microhardness and determination of the mechanical properties of the superconducting samples (Lu0.1, Lu0.3, Lu0.5 and Lu0.7) exhibiting the ISE behavior. However, for the undoped sample obtaining RISE nature, the models used above are not successful enough to describe the microhardness values close to those of the plateau region. Thus, Indentation-Induced Cracking (IIC) Model, except for these models, will be used to analyze the mechanical properties of the pure sample with the RISE behavior.

3.6 Analysis using indentation-induced cracking (IIC) model

The Indentation-Induced Cracking (IIC) model is used for the microhardness analysis of the materials exhibiting RISE behavior [44]. According to the model, at the maximum depth the applied load is balanced by the total sample

resistance consisting of four components: (1) The slipping of the indenter or the specimen at the interfaces. (2) Elastic deformation. (3) Plastic deformation. (4) Cracks/voids in the material.

1st and 2nd components are the basic reason for the ISE behaviour whereas the RISE nature of the material results from the indentation cracks/voids [44]. The load independent microhardness value (H_{IIC}) can be computed using the following equation:

$$H_v = \lambda_1 K_1 \left(\frac{F}{d^2} \right) + K_2 \left(\frac{F^{5/3}}{d^3} \right) \quad (12)$$

where λ_1 , K_1 and K_2 are constants. The constant K_1 value changes with the indenter geometry and K_2 depends on the applied load. For a perfect plastic material $H_v = K_1 \left(\frac{F}{d^2} \right)$, $\lambda_1 = 1$ and $H_v = K_2 \left(\frac{F^{5/3}}{d^3} \right) = 0$, whereas for ideal brittle solids $H_v = K_2 \left(\frac{F^{5/3}}{d^3} \right)$ and $\lambda_1 = 0$.

For Eq. 12, the indentation diagonal size is supposed to be $d = 7h$ due to the angle of 148° between the opposite sides of the indenter and h denotes the depth of the indentation. The second part of Eq. 12 is used for brittle materials such as the Lu-doped bulk Y123 superconductors. Hence, Eq. 12 can be rewritten as following formula:

$$H_v = K \left(\frac{F^{5/3}}{d^3} \right)^m \quad (13)$$

where K and m denote load independent constants, respectively. The variation of microhardness value $\ln(H_v)$ with $\ln(F^{5/3}/d^3)$ for all the samples is given in Fig. 6. The extracted values of K and m are illustrated in Table 7. The

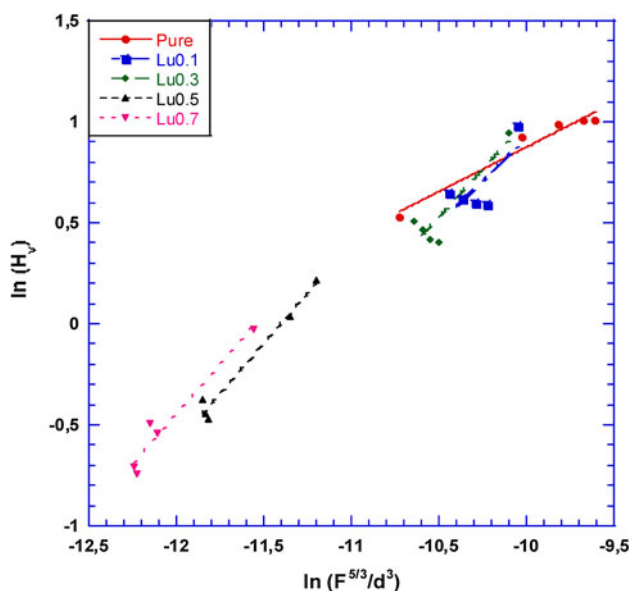


Fig. 6 Variation of $\ln H_v$ with $\ln(F^{5/3}/d^3)$ according to *IIC* model for all samples

Table 7 Best-fit results of experimental data according to *IIC* model

Samples	$K \times 10^4$ ($N^{(3-5m)/3}/\mu m^{(2-3m)}$)	m	H_{IIC} (GPa)	H_v (GPa)
Pure	5.28	0.44	2.601	2.680–2.742
Lu0.1	9.45	0.85	2.062	1.804–1.854
Lu0.3	10.53	0.95	1.808	1.498–1.591
Lu0.5	11.31	0.99	0.862	0.622–0.687
Lu0.7	11.43	0.98	0.702	0.475–0.580

Table 8 The results of load dependent Vickers microhardness at the plateau region and load independent hardness values calculated using *PSR*, *EPD*, *HK* and *IIC* models

Samples	H_v (GPa) (in plateau region)	H_{PSR} (GPa)	H_{EPD} (GPa)	H_{HK} (GPa)	H_{IIC} (GPa)
Pure	2.680–2.742	3.152	3.117	2.833	2.601
Lu0.1	1.804–1.854	1.576	1.559	1.762	2.062
Lu0.3	1.498–1.591	1.223	1.253	1.452	1.808
Lu0.5	0.622–0.687	0.426	0.474	0.587	0.862
Lu0.7	0.475–0.580	0.352	0.363	0.452	0.702

m values can be used to describe the type of ISE behaviour for $m > 0.6$ whereas $m < 0.6$ points out the RISE behaviour [41, 45]. One can see from Table 7, the power m value is obtained to be about 0.85, 0.95, 0.99 and 0.98 for the Lu0.1, Lu0.3, Lu0.5 and Lu0.7 samples, respectively whereas the value of m is found to be about 0.44 for the Lu0.0 sample, meaning that the Lu-doped samples exhibit the ISE feature while the pure sample obeys the RISE behavior. In other words, the Lu inclusions in the Y123 matrix damage the RISE behaviour and favor the ISE performance of the bulk superconducting samples.

To sum up, the *IIC* model gives the most correct hardness results for the pure material exhibiting the RISE behavior due to the lack of the elastic deformation in the material whereas *HK* approach is found to be the best model to explain the microhardness values of the Lu-doped samples exhibiting the ISE behavior due to the degradation in the mechanical properties. These results are clearly summarized in Table 8.

4 Conclusion

In this study, the effect of Lu inclusions on the mechanical properties of the $YBa_2Lu_xCu_3O_{7-\delta}$ superconducting samples prepared by the liquid ammonium nitrate and derivatives with $x = 0, 0.1, 0.3, 0.5$ and 0.7 is researched by means of the microhardness measurements. The experimental results are used to determine the Vickers microhardness, Young's modulus, yield strength and fracture

toughness values, being account for the potential industrial applications of the superconducting materials. It is observed that the all the values estimated above degrade with the Lu addition in the system as a consequence of the decrement in the connectivity between superconducting grains. Moreover, the pure sample exhibits the RISE behavior being explained by the linear variable of microhardness while the others obey the ISE feature being described by the non-linear changeable in the microhardness. Additionally, the Vickers microhardness results allow us to derive the mechanical properties of the undoped and Lu-doped Y123 superconducting samples using the Meyer's law, proportional sample resistance, Elastic–Plastic deformation, Hays–Kendall and Indentation-Induced Cracking model. Based on the results obtained from the theoretical calculations, Hays–Kendall approach produces successful results for the pure sample exhibiting the ISE behavior whereas the IIC model successfully explains RISE nature for the other samples, presenting the degradation in the mechanical properties with the Lu individuals in the Y123 system. Further, the most striking feature of the paper is the fact that both the elastic and plastic deformations are observed in the pure sample while the plastic deformation becomes more and more dominant compared to the elastic deformation in the Lu-doped superconductors.

Open Access This article is distributed under the terms of the Creative Commons Attribution License which permits any use, distribution, and reproduction in any medium, provided the original author(s) and the source are credited.

References

- M.E. Sagsoz, M. Ertugrul, U. Cevik, *Mater. Lett.* **60**, 1778 (2006)
- K. Wu, J.R. Ashburn, C.J. Torng, P.H. Hor, R.L. Meng, L. Gao, Z.J. Huang, Y.Q. Wang, C.W. Chu, *Phys. Rev. Lett.* **58**, 908 (1987)
- P. Bordet, C. Chaillout, J. Chenavas, J.L. Hodeau, M. Marezio, J. Karpinski, E. Kaldis, *Nature* **336**, 596 (1988)
- P. Marsh, R.M. Fleming, M.L. Mandich, A.M. DeSantolo, J. Kwo, M. Hong, L.J. Martinez-Miranda, *Nature* **334**, 660 (1988)
- C. Terzioglu, M. Yilmazlar, O. Ozturk, E. Yanmaz, *Physica C* **423**, 1190 (2005)
- C. Terzioglu, O. Ozturk, A. Kilic, A. Gencer, I. Belenli, *Physica C* **434**, 153 (2006)
- S. Gupta, R.S. Yadav, N.P. Lalla, G.D. Verma, B. Das, *Integr. Ferroelectr.* **116**, 68 (2010)
- P.M. Sarun, S. Vinu, R. Shabna, A. Biju, U. Syamaprasad, *Mater. Res. Bull.* **44**, 1017 (2009)
- O. Ozturk, M. Akdogan, H. Aydin, M. Yilmazlar, C. Terzioglu, I. Belenli, *Phys. B* **399**, 94 (2007)
- B. Batlogg, *Solid State Commun.* **107**, 639 (1998)
- A. Kuczowski, B. Kusz, *Synth. Met.* **94**, 145 (1998)
- O. Gorur, G. Yildirim, S.P. Altintas, C. Terzioglu, *J. Mater. Sci.: Mater. Electron.* (2012). doi:10.1007/s10854-012-1022-0
- J. Gong, J. Wu, Z. Guan, *J. Eur. Ceram. Soc.* **19**, 2625 (1999)
- J. Gong, Z. Zhao, Z. Guan, H. Miao, *J. Eur. Ceram. Soc.* **20**, 1895 (2000)
- J. Gong, Y. Li, *J. Mater. Sci.* **35**, 209 (2000)
- C. Hays, E.G. Kendall, *Metallography* **6**, 275 (1973)
- D.R. Tate, *Trans Am Soc Metals AIME* **35**, 374 (1945)
- S.J. Bull, T.F. Page, E.H. Yoffe, *Phil Mag Lett* **59**, 281 (1989)
- G.P. Upit, S.A. Varchenya, *Phys Stat Sol* **17**, 831 (1986)
- R.M. Ren, Z.G. Yang, L. Shaw, *J. Am. Ceram. Soc.* **85**, 819 (2002)
- H. Gao, Y. Huang, *Scripta Mater.* **48**, 113 (2003)
- D. Beegan, S. Chowdhury, M.T. Laugier, *Surf Coat Tech* **176**, 124 (2003)
- M.B. Turkoz, S. Nezir, C. Terzioglu, A. Varilci, G. Yildirim, *J. Mater. Sci.: Mater. Electron.* (2012). doi:10.1007/s10854-012-0846-y
- M.B. Turkoz, S. Nezir, A. Varilci, G. Yildirim, M. Akdogan, C. Terzioglu, *J. Mater. Sci.: Mater. Electron.* (2012). doi:10.1007/s10854-012-0967-3
- S.M. Khalil, *J. Phys. Chem. Solids* **64**, 855 (2003)
- H. Maeda, Y. Taraka, *Jpn Appl Phys* **27**, L209 (1987)
- S. Vinu, P.M. Sarun, R. Shabna, A. Biju, U. Syamaprasad, *Mater. Chem. Phys.* **119**, 135 (2010)
- A. Biju, U. Syamaprasad, A. Rao, J.G. Xu, K.M. Sivakumar, Y.K. Kuo, *Physica C* **466**, 69 (2007)
- R. Shabna, P.M. Sarun, S. Vinu, A. Biju, U. Syamaprasad, *Supercond. Sci. Technol.* **22**, 045016 (2009)
- O. Sahin, O. Uzun, U. Kolemen, N. Ucar, *Mater. Charact.* **58**, 197 (2007)
- C. Terzioglu, *J. Alloy, Compound* **509**, 87 (2011)
- O. Ozturk, E. Asikuzun, M. Erdem, G. Yildirim, O. Yildiz, C. Terzioglu, *J. Mater. Sci.: Mater. Electron.* **23**, 511 (2012)
- E. Asikuzun, O. Ozturk, H.A. Cetinkara, G. Yildirim, A. Varilci, M. Yilmazlar, C. Terzioglu, *Mater. Sci. Mater. Electron* **23**, 1001 (2012)
- M.F. Azzouz, A. Mchirgui, B. Yangui, C. Boulesteix, B.M. Salem, *Physica C* **356**, 83 (2001)
- K. Kocabas, S. Sakiroglu, M. Ciftcioglu, I. Ercan, H. Epik, O. Bilgili, *J. Supercond. Nov. Magn* **22**, 749 (2009)
- M. Dogruer, G. Yildirim, O. Ozturk, A. Varilci, N. Soylu, O. Gorur, C. Terzioglu, *Mater. Sci. Mater. Electron* (2012). doi:10.1007/s10854-012-0917-0
- T. Kucukomeroglu, E. Bacaksiz, C. Terzioglu, A. Varilci, *Thin Solid Films* **516**, 2913 (2008)
- A. Biju, P.M. Sarun, R.P. Aloysius, U. Syamaprasad, *J. Alloy, Compound* **454**, 46 (2008)
- N. Gane, F.P. Bowden, *J. Appl. Phys.* **39**, 1432 (1968)
- R. Awad, A.I. Abou-Aly, M. Kamal, M. Anas, *J. Supercond. Nov. Magn* **24**, 1947 (2011)
- J.B. Quinn, V.D. Quinn, *J. Mater. Sci.* **32**, 4331 (1997)
- Z. Peng, J. Gong, H. Miao, *J. Eur. Ceram. Soc.* **24**, 2193 (2004)
- O. Ozturk, C. Terzioglu, I. Belenli, *J. Supercond. Nov. Magn* **24**, 381 (2011)
- H. Li, R.C. Bradt, *J. Mater. Sci.* **31**, 1065 (1996)
- K. Sangwal, *Mater. Chem. Phys.* **63**, 145 (2000)